International Journal of Thermophysics, Vol. 5, No. 1, 1984

Measurements of Thermophysical Properties by a Stepwise Heating Method

N. Araki[1]

Received February 8, 1984

An outline of the stepwise heating method for measuring thermal diffusivity and specific heat capacity of samples in both solid and liquid phases is described. The method is based on the measurement of temperature response at the surface of a solid sample when the other surface is heated in step-function. By making the best use of the characteristic points of this method, applications to samples in the liquid state, especially to high temperature melts such as molten salts, have been tried. As examples of measurement results, the thermal diffusivity, specific heat capacity, and thermal conductivity of zirconia brick and the thermal diffusivity of molten salts are shown in graphic form.

KEY WORDS: molten flouride salt; stepwise heating method; specific heat capacity; thermal diffusivity; zirconia brick.

1. INTRODUCTION

The stepwise heating method for measuring thermal diffusivity and specific heat capacity of a disk-shaped solid specimen was developed by Kobayasi and Kumada [1–3]. Measurements in the temperature range above 500 K were corrected for radiation heat loss from all surfaces of the disk-shaped specimen on the basis of theoretical considerations [4]. Recently, in order to obtain more accurate data of specific heat capacity, the stepwise heating method has been improved by the use of the single rectangular pulse heating method [5]. Furthermore, the measuring apparatus was adapted for automatic measurement in the high temperature range up to 1500 K [6].

Application of the stepwise heating method to samples in the liquid phase has been made by Kobayasi, Araki, Kato, and others [7–12]. Ini-

Presented at the Japan–United States Joint Seminar on Thermophysical Properties, October 24–26, 1983, Tokyo, Japan.

[1] Department of Mechanical Engineering, Shizouka University, Hamamatsu 432, Japan.

0195-928X/84/0300-0053$03.50/0

tially, it was assumed that the infinite plane heat source (a stainless steel plate of 0.1 mm in thickness) is placed in the infinite media of a liquid sample [7, 8]. In order to prevent occurrence of natural convection in the sample liquid, a method for applying the sample as a thin layer was developed [9]. A metallized ceramic cell with a thin alumina coating to insulate it electrically from the sample has been developed [10, 17]. An alternative method uses a three layered cell, which is heated in step-function by thermal radiation [11, 12, 19].

Cowan [13] conducted theoretical studies with a stepwise, pulsewise, and periodic heating method for determining thermal diffusivity. His conclusion was that the stepwise heating method would probably yield poor results. On the other hand, the laser-flash method, which was proposed by Parker et al. [14], has been intensively adopted by many researchers. However, it is not possible to eliminate the comparatively large errors arising from uneven distribution of the laser beam as the incident radiation heat source [15]. The stepwise heating method would be able to use heating sources with low energy density such as a tungsten lamp, a xenon arc lamp, and a metal plate with Joulean heating. This is due to the fact that, even with these low density energy sources, the signal of temperature response is high enough to be measured because of the long heating duration (5–10 s). These heating sources have many advantages as follows. First, the temperature difference between the heating surface and the measuring surface can be kept small, so these sources can be used successfully for a liquid sample near the boiling temperature, and for a sample whose properties have strong temperature dependency. Second, a more extensive surface area can be uniformly heated, i.e., the one-dimensional concept can be realized, so these sources are advantageous for a sample in liquid or gaseous state where a container is needed. Finally, these sources are inexpensive and easily available in comparison with a laser-flash method.

2. STEPWISE HEATING METHOD FOR SOLID SAMPLES

2.1. Principle of the Measuring Method of Thermal Diffusivity

Theoretical and experimental studies on the stepwise heating method of measuring thermal diffusivity of a small disk were made by Kobayasi and Kumada [1]. If the thickness of a solid disk is large enough in comparison with its diameter, the problem can be simplified to solving the heat conduction in a slab. The correction to the radiation heat loss from all surfaces of the disk was studied [4], but in the present paper a one-dimensional treatment as shown in Fig. 1 is discussed.

When a sample is placed within a vacuum furnace and the front surface is subjected to stepwise heating by thermal radiation with heat flux

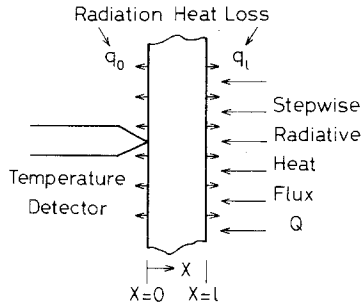

Fig. 1. Schematic diagram of a sample in the solid phase (infinite slab).

Q, the resulting temperature response at the rear surface is expressed by the following equation:

$$\Theta = \frac{\theta(0,t)}{Ql/\lambda} = \frac{1}{\alpha+\beta} - 2\sum_{\kappa=0}^{\infty} \frac{\exp(-at\gamma_\kappa^2/l^2)}{D_\kappa} \tag{1}$$

where

$$D_\kappa = \gamma_\kappa \sin\gamma_\kappa \left(1 + \alpha - \frac{2\beta}{\alpha} + \frac{\gamma_\kappa^2}{\alpha+\beta} + \frac{\beta}{\gamma_\kappa^2} + \frac{\beta^2}{\alpha\gamma_\kappa^2}\right) \tag{2}$$

$$R_0 = 4\epsilon_0\sigma T_0^3/\lambda, \qquad R_l = 4\epsilon_l\sigma T_0^3/\lambda \tag{3}$$

$$\alpha = (R_0 + R_l)l = R_0 l\{1 + (\epsilon_l/\epsilon_0)\} \tag{4}$$

$$\beta = R_0 R_l l^2 = (R_0 l)^2(\epsilon_l/\epsilon_0) \tag{5}$$

and a is the thermal diffusivity, l is the thickness of the sample, Q is the rate of heat absorption at the front surface of the sample, and q is the rate of heat loss expressed as follows:

$$q = \epsilon\sigma\{(T_0+\theta)^4 - T_0^4\} \simeq 4\epsilon\sigma T_0^3\theta$$

Also, T_0 is the initial temperature in K, t is the time variable, ϵ is the equivalent emissivity including the shape factor, θ is the temperature rise, Θ is the dimensionless temperature rise, λ is the thermal conductivity, σ is Stefan–Boltzmann's constant, and the subscripts 0 and l denote the quantities at the rear and the front surface, respectively. Finally, γ_κ is the kth root,

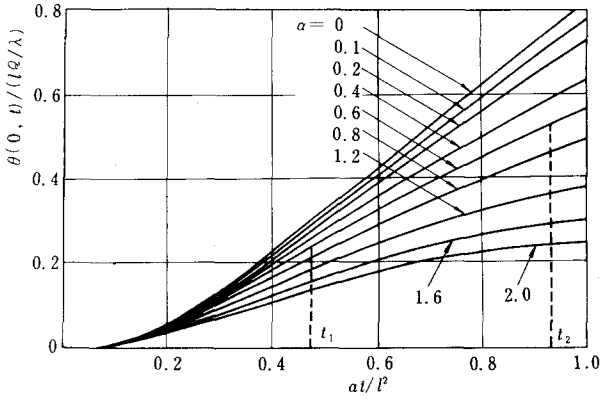

Fig. 2. Dimensionless temperature rise at the rear surface of the slab.

which is determined by the following eigenvalue equation:

$$\cot\gamma = \frac{\gamma}{\alpha} - \frac{\beta}{\alpha\gamma} \tag{6}$$

Figure 2 represents the dimensionless temperature rise for Eq. (1) with the

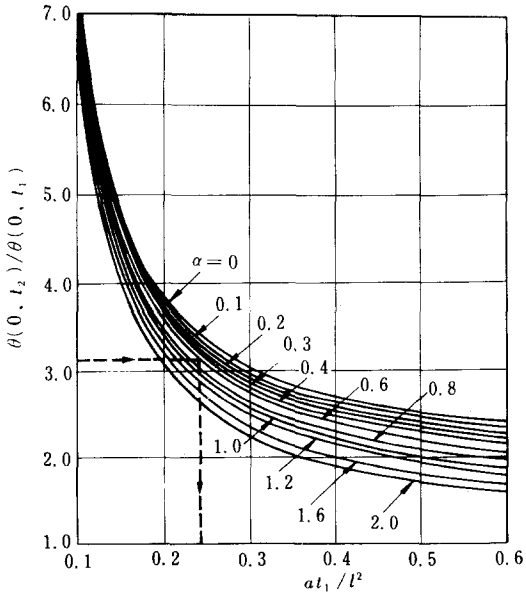

Fig. 3. Temperature ratio vs Fourier number for the infinite solid slab.

radiation heat loss parameter α. The curve corresponding to $\alpha = 0$ is the case of no radiation heat loss from the surfaces. Actually, the value of α can be neglected at temperatures below 650 K.

The unknown values of Q and λ contained in the temperature response can be eliminated by introducing the ratio of temperature at times t_1 and t_2. Figure 3 shows the temperature ratio $\theta(0, 2t_1)/\theta(0, t_1)$ against Fourier number ($Fo = at_1/l^2$). The temperature ratio is determined experimentally without knowing the absolute temperature values. When this ratio is obtained experimentally and the proper value of the parameter α is given, the Fourier number, i.e., the thermal diffusivity, is determined because the thickness l and time t_1 are known values. As the parameter α is a function of the thermal diffusivity, a proper value of α is given by an iterative procedure and other methods [1].

2.2. Principle of the Measuring Method of Specific Heat Capacity

In the ideal case of a perfectly insulated sample ($\alpha = 0$), the temperature rise of the rear surface changes linearly with time for the range of $Fo > 0.5$. Hence, the specific heat capacity can be determined by comparing the observed temperature rise with that of a standard sample as follows:

$$c = \frac{(\theta_{s^2} - \theta_{s^1})}{(\theta_2 - \theta_1)} \cdot \frac{(t_2 - t_1)}{(t_{s^2} - t_{s^1})} \cdot \frac{\rho_s l_s}{\rho l} c_s \tag{7}$$

where c is the specific heat capacity, ρ is the density, the subscripts 1 and 2 correspond to the quantities at the different times t_1 and t_2, respectively, and the subscript s refers to the standard sample while the surfaces of both samples have the same treatment so as to obtain equal emissivity. At higher temperatures the correction due to radiation heat loss from the surfaces is needed as follows:

$$c = \frac{\Delta\theta_s}{\Delta\theta} \cdot \frac{\Delta t}{\Delta t_s} \cdot \frac{\rho_s l_s}{\rho l} \cdot \frac{M_s}{M} c_s \tag{8}$$

$$M = \frac{\Delta\theta}{\Delta\theta_r}, \qquad M_s = \frac{\Delta\theta}{\Delta\theta_{sr}} \tag{9}$$

where the subscript r denotes the quantity with heat loss, and the correction factor M is calculated as a function of Fo with the parameter α [3]. The single rectangular pulse heating method [5] has been developed to obtain more accurate data for the specific heat capacity as shown in Fig. 4. From the first half of the temperature response the thermal diffusivity is obtained, and the specific heat capacity is determined from the known heat flux

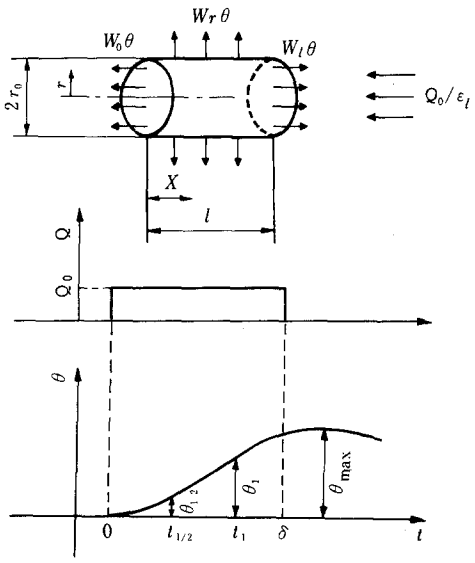

Fig. 4. Principle of the single rectangular pulse heating method.

during the time duration δ and the observed maximum temperature rise θ_{max}.

2.3. Measuring Apparatus and Procedure

Figure 5 shows a block diagram of the measuring apparatus [6]. A sample is shaped into a disk of about 12 mm in diameter and 2–15 mm in thickness depending on the value of the thermal diffusivity. The surfaces of the specimen are coated with an electroconductivity paint to keep absorptivity of the surfaces constant and to make temperature measurement easy. The specimen is mounted in a vacuum furnace and subjected to a single rectangular pulse heating by a xenon-arc lamp through a mechanical shutter which controls the pulse width. The temperature response of the rear surface is detected by a fine thermocouple and amplified after canceling the electromotive force of the initial temperature by a compensator, and then it is recorded digitally into a memory. A microcomputer connected to the memory is used to calculate the thermal diffusivity and the specific heat capacity simultaneously.

2.4. Experimental Results

As an example of the measured results, the thermal diffusivity and specific heat of a zirconia brick composed mainly of ZrO_2 and SiO_2 are shown in Figs. 6 and 7, respectively. The thermal conductivity, which was

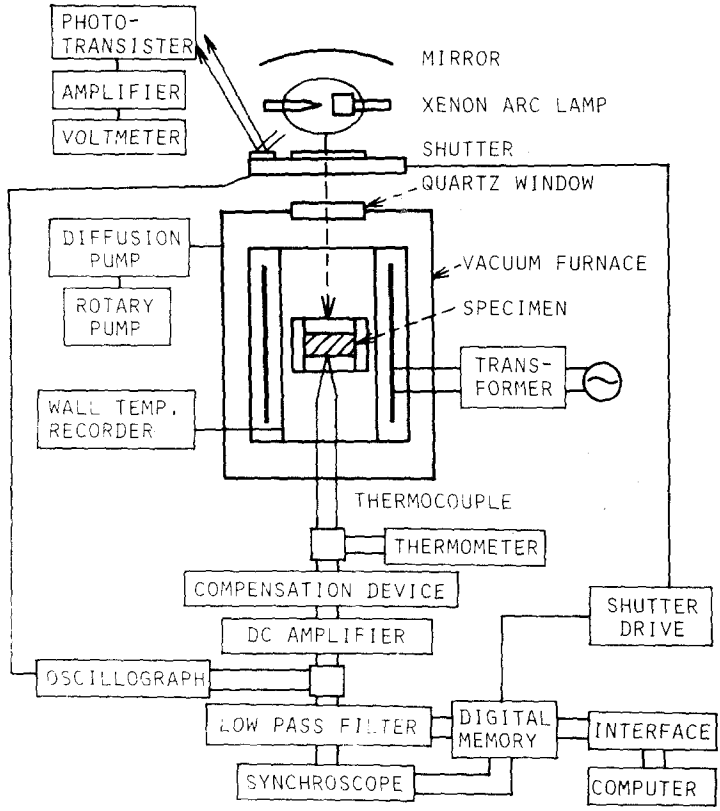

Fig. 5. Block diagram of measuring apparatus for the single rectangular pulse heating method.

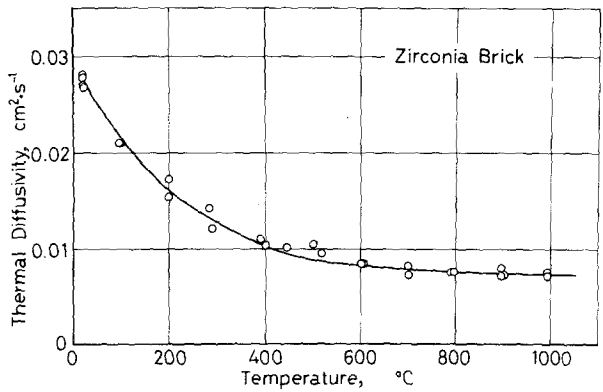

Fig. 6. Thermal diffusivity of zirconia brick.

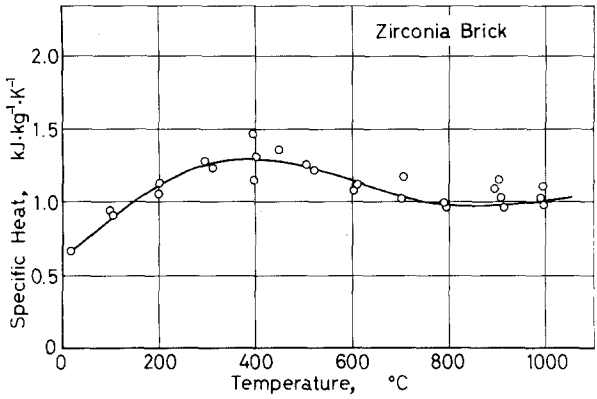

Fig. 7. Specific heat capacity of zirconia brick.

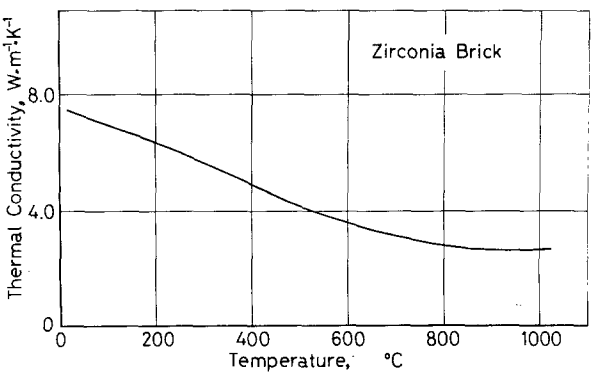

Fig. 8. Thermal conductivity of zirconia brick.

calculated from the product of the thermal diffusivity, specific heat capacity, and density ($\rho = 365$ kg · m^{-3}), is shown in Fig. 8.

3. STEPWISE HEATING METHOD FOR LIQUID SAMPLES WITH A METALLIZED CERAMIC CELL

3.1. Principle of the Measuring Method

One-dimensional heat flow [9] through infinite parallel planes is considered as shown in Fig. 9, where a sample liquid *1* is contained in the thin layer between the bottom material *2* and the upper heating plate *3*. When

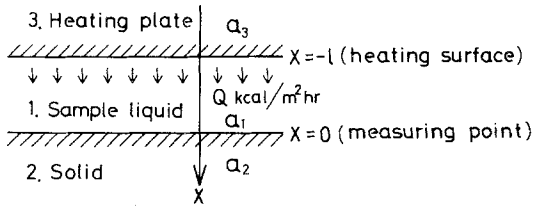

Fig. 9. Schematic diagram of a liquid sample contained in a thin layer.

the upper surface of the sample liquid is heated in a stepwise manner by the heating plate, the temperature response at the bottom of the liquid layer is expressed as follows:

$$\Theta = \frac{\theta_1(0,t)}{Ql/\lambda} = (1+\delta)\cdot\sum_{n=0}^{\infty}\delta^n\left\{\frac{2\sqrt{Fo}}{\sqrt{\pi}}\cdot\exp\left(-\frac{(2n+1)^2}{4Fo}\right)\right.$$

$$\left.-(2n+1)\mathrm{erfc}\left(\frac{2n+1}{2\sqrt{Fo}}\right)\right\} \qquad (10)$$

where

$$Fo = a_1 t/l^2, \qquad (11)$$

and

$$\delta = (1-\phi)/(1+\phi), \qquad \phi = \sqrt{\lambda_2\rho_2 c_2/\lambda_1\rho_1 c_1} \qquad (12)$$

The right-hand side of Eq. (10), namely, the dimensionless temperature rise, is expressed as a function of Fo with δ as a parameter as shown in Fig. 10. In order to eliminate the generating heat flux Q, we take a temperature ratio $\theta_1(0,2t_1)/\theta_1(0,t_1)$ as shown in Fig. 11, where Fourier number is defined with t_1 as $Fo = a_1 t_1/l^2$.

In an experimental procedure, when a temperature ratio is obtained from a curve of the temperature rise at the bottom of the sample layer, the value of Fo can be found as a function of δ. The value of δ is in the region of $-1 < \delta < 1$ depending on the thermophysical properties of the sample liquid and the bottom material. In Fig. 11 we note that the effect of δ on Fo is negligibly small in the region of $Fo < 0.3$. Therefore, we may determine Fo by using the curve of $\delta = 0$, which means that the bottom material has

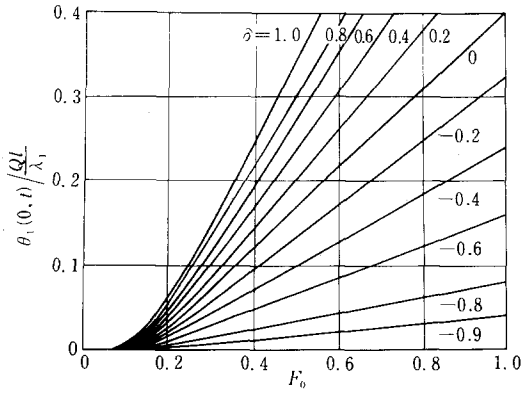

Fig. 10. Dimensionless temperature rise of a liquid sample in a thin layer.

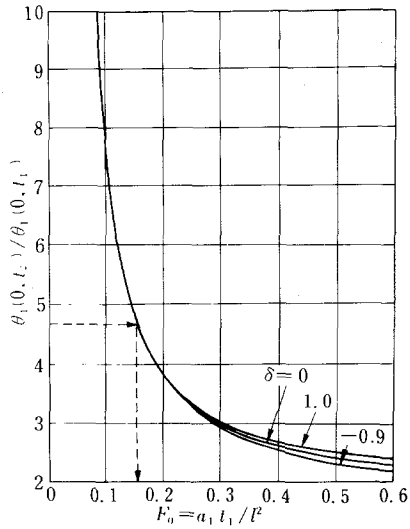

Fig. 11. Temperature ratio vs Fourier number for a liquid sample in a thin layer.

properties equal to those of the sample liquid. This *Fo* value directly gives the thermal diffusivity of the sample.

3.2. Measuring Apparatus

Figure 12 shows the ceramic cell which has metallized layers as the heat source and a resistance thermometer to measure the temperature

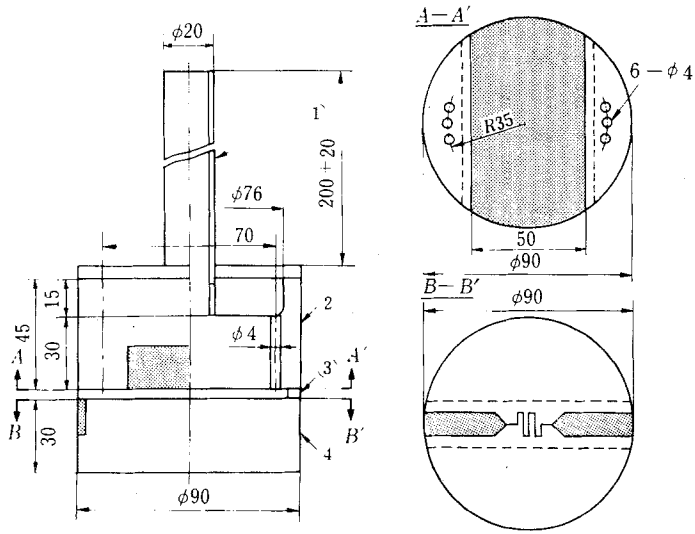

Fig. 12. Metallized ceramic cell with alumina coating.

response. The thickness and radius of both the upper part *2* and the lower part *4*, which correspond to the layers *1* and *3* in Fig. 9, are 30 and 45 mm, respectively. It is confirmed by the theoretical analysis [21] that the cell has a sufficient size for the application of Eq. (10).

Each part of the cell is made of pure alumina and is glued together by the same kind of alumina cement. A molten salt as a sample liquid is applied as a thin layer between the upper part *2* and the lower part *4*. On the bottom surface of part *2* (cross-section $A-A'$), the thin platinum layer of 50 mm width and 0.015 mm thickness is metallized as the plane heat source. On the upper surface of part *4* (cross-section $B-B'$), the platinum resistance thermometer of 0.015 mm in thickness is metallized. These metallized layers are coated, respectively, by thin alumina layers of about 0.02 mm thickness for electrically insulating the sample salt. The effect of these coating layers on the theoretical curves was estimated and compensated for in the computer program of the data processing [17].

The coating technique, the thin alumina layer on the metallized layer, and the adhesive materials for gluing each ceramic part of the cell had been improved step by step. The improved ceramic cell was expected to have better compatibility with molten fluoride salts. A sample salt at room temperature is put into the cell through the tube *1*, and then is melted in an electric furnace. The tube prevents wetting along outer surfaces of the cell by the salt vapor during its melting.

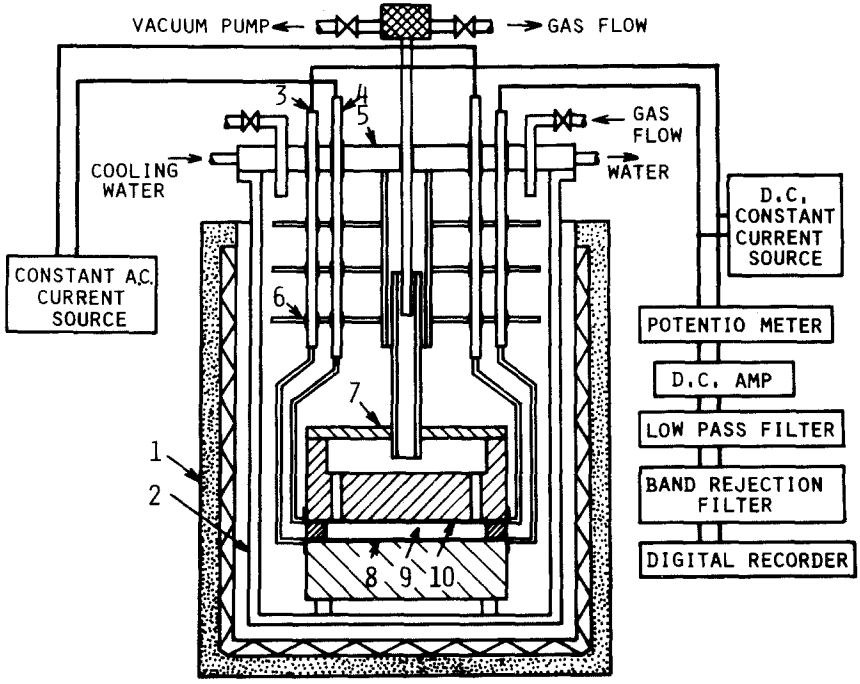

Fig. 13. Schematic diagram of the measuring apparatus using the ceramic cell: *1*, electric furnace; *2*, container; *3*, *4*, electrode; *5*, water jacket (lid); *6*, radiation shield plate; *7*, ceramic cell; *8*, resistance thermometer; *9*, sample salt; *10*, heating source.

A schematic diagram of the measuring apparatus with this cell is shown in Fig. 13. Two sets of electrodes, *3* and *4*, are used for the resistance thermometer and for the heat source supply. Just below its melting point, the sample is dried for long time in a He gas atmosphere and under reduced gas pressure. When the metallized layer, *10*, is heated in a stepwise manner by the electric current, the resulting temperature history is measured by the resistance thermometer, *8*, and recorded digitally into a memory, and then the data are processed by a computer.

3.3. Measured Results

In Fig. 14 an example of the measured results is shown for a molten fluoride salt (Li_2BeF_4, Flibe) [17]. The values by Cooke are converted from the measured thermal conductivity data [18]. The other example is shown in Fig. 15 for the molten fluoride salt containing thorium ($LiF–BeF_2–ThF_4$, 67–18–15 mol%) [21].

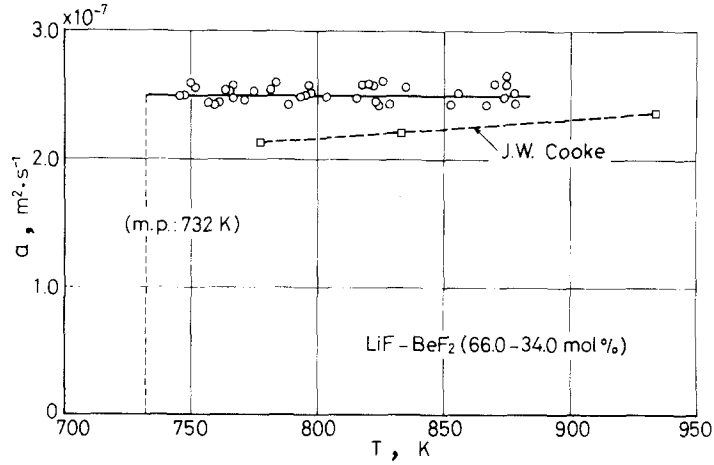

Fig. 14. Thermal diffusivity of molten fluoride sale (Flibe).

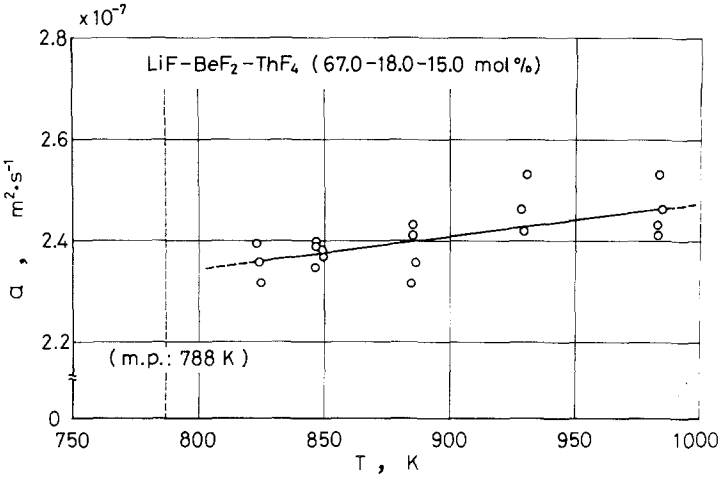

Fig. 15. Thermal diffusivity of molten fluoride salt containing thorium.

4. STEPWISE HEATING METHOD FOR LIQUID SAMPLES WITH A THREE LAYERED CELL

4.1. Principle of the Measuring Method

In Fig. 16, a three layered cell is considered. A sample liquid is contained in the central layer, whereas the first and third layers are

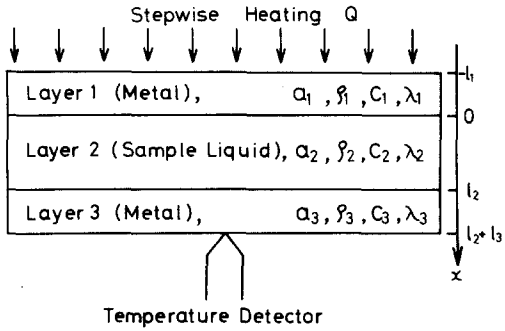

Fig. 16. Schematic diagram of liquid sample cell (the three layered-cell).

composed of metal plates as a container. When the front surface of the cell is subjected to a stepwise radiation energy, the resulting temperature history at the rear surface is expressed as a function of the thermal diffusivity, specific heat capacity, density, and thickness of the three layered composites as follows:

$$\theta_3(l_2 + l_3, t) = \frac{(2Ql_2/\lambda_2)(\eta_{3/2})^2}{3H_{3/2}}$$

$$\left[\frac{\left\{ 6\frac{Fo_2}{(\eta_{3/2})^2} \right\}(X_1\omega_1 + X_2\omega_2 + X_3\omega_3 + X_4\omega_4) - (X_1\omega_1^3 + X_2\omega_2^3 + X_3\omega_3^3 + X_4\omega_4^4)}{(X_1\omega_1 + X_2\omega_2 + X_3\omega_3 + X_4\omega_4)^2} \right.$$

$$\left. - \sum_{\kappa=1}^{\infty} \frac{12\exp\left(-\gamma_\kappa^2 \frac{Fo_2}{\eta_{3/2}^2} \right)}{\gamma_\kappa^2 \{ X_1\omega_1\cos(\omega_1\gamma_\kappa) + X_2\omega_2\cos(\omega_2\gamma_\kappa) + X_3\omega_3\cos(\omega_3\gamma_\kappa) + X_4\omega_4\cos(\omega_4\gamma_\kappa) \}} \right] \tag{13}$$

Here Fo_2 is the Fourier number based on the second layer ($Fo = a_2 t / l_2^2$), H is the heat capacity ($H = c\rho l$), η is the square root of heat diffusion time

($\eta = \sqrt{l^2/a}$), and γ_κ is the κth positive root of the following equation:

$$X_1 \sin(\omega_1 \gamma) + X_2 \sin(\omega_2 \gamma) + X_3 \sin(\omega_3 \gamma) + X_4 \sin(\omega_4 \gamma) = 0 \tag{14}$$

where

$$X_1 = H_{1/3}\eta_{3/1} + H_{1/2}\eta_{2/1} + H_{2/3}\eta_{3/2} + 1 \tag{15}$$

$$X_2 = H_{1/3}\eta_{3/1} - H_{1/2}\eta_{2/1} + H_{2/3}\eta_{3/2} - 1 \tag{16}$$

$$X_3 = H_{1/3}\eta_{3/1} + H_{1/2}\eta_{2/1} - H_{2/3}\eta_{3/2} + 1 \tag{17}$$

$$X_4 = H_{1/3}\eta_{3/1} + H_{1/2}\eta_{2/1} - H_{2/3}\eta_{3/2} - 1 \tag{18}$$

$$\omega_1 = \eta_{1/3} + \eta_{2/3} + 1 \tag{19}$$

$$\omega_2 = \eta_{1/3} + \eta_{2/3} - 1 \tag{20}$$

$$\omega_3 = \eta_{1/3} - \eta_{2/3} + 1 \tag{21}$$

$$\omega_4 = \eta_{1/3} - \eta_{2/3} - 1 \tag{22}$$

The subscripts 1, 2, 3 denote the layer number of the cell, and the subscripts i/k ($i, k = 1, 2, 3$) refer to (quantity of the ith layer)/(quantity of kth layer). Also from Eq. (13),

$$\theta_3(l_2 + l_3, t)/(Ql_2/\lambda_2) = \Theta$$

is the dimensionless temperature response. An example of the response is shown in Fig. 17 when the first and third layer have the same material and

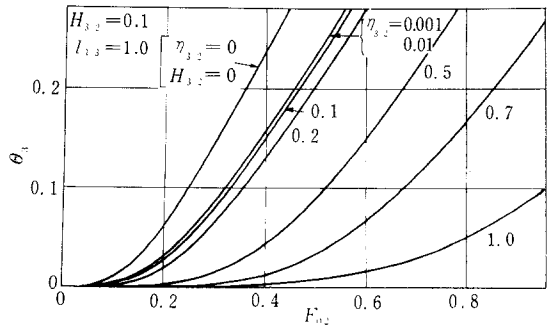

Fig. 17. Dimensionless temperature rise of the three layered cell.

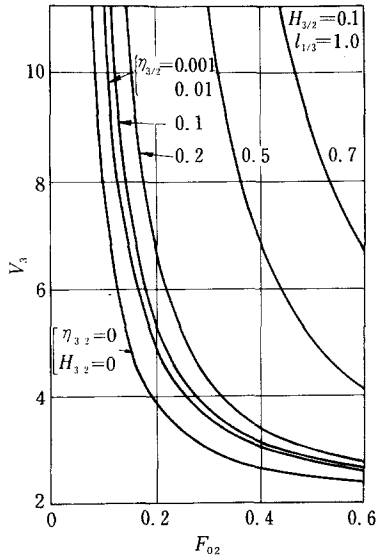

Fig. 18. Ratio of temperature vs Fourier number for the three layered cell.

thickness, respectively. In the figure, $H_{3/2} = 0$, $\eta_{3/2} = 0$ correspond to the case where only a single layer exists, the second layer.

By considering the ratio of temperature rises at different times, the heat quantity Q is eliminated. The temperature ratio is expressed as the function of $H_{i/k}$, $\eta_{i/k}$, and Fo_2 as shown in Fig. 18. When the temperature ratio is measured experimentally and the thermophysical properties of each layer except the thermal diffusivity of the central layer are given, the unknown thermal diffusivity of the sample can be calculated by comparison with the theoretical temperature ratio [11]. This procedure requires the known value of the specific heat capacity of the sample and the known thermal properties of the cell wall. So, the extrapolation method, which does not require these properties, has been proposed [19]. The degree of errors due to heat loss from the surfaces of the cell has been analyzed, and a method for correction of these errors has been proposed [12].

4.2. Measuring Apparatus

A schematic diagram of the measuring apparatus is shown in Fig. 19. A sample salt in a pot, *10*, is fused by an electric furnace, *11*. After melting, the sample salt is supplied to the cell, *8*, by opening a valve. The front surface of the cell is subjected to stepwise radiation from an iodine lamp, *4*, through a mechanical shutter, *6*. The resulting temperature history is

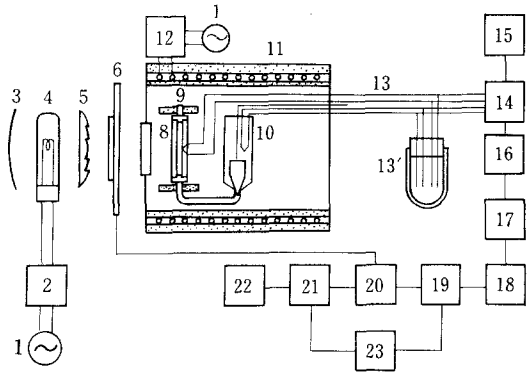

Fig. 19. Schematic diagram of the measuring apparatus using the three layered cell: *1*, power source; *2*, transformer; *3*, concave mirror; *4*, iodine lamp; *5*, fresnel lens; *6*, shutter; *7*, quartz window; *8*, three layered cell; *9*, shroud; *10*, pot; *11*, electric furnace; *12*, controller; *13*, thermocouple; *14*, *19*, *21*, transfer switch; *15*, potentiometer; *16*, nul-adjuster; *17*, amplifier; *18*, filter; *20*, digital memory; *21*, chart recorder; *23*, oscilloscope.

recorded digitally into a memory, *20*, and the data are processed by a computer.

4.3. Measured Results

As an example of the measured results, the thermal diffusivity of sodium nitrate is shown in Fig. 20 [12]. The values of the data are almost

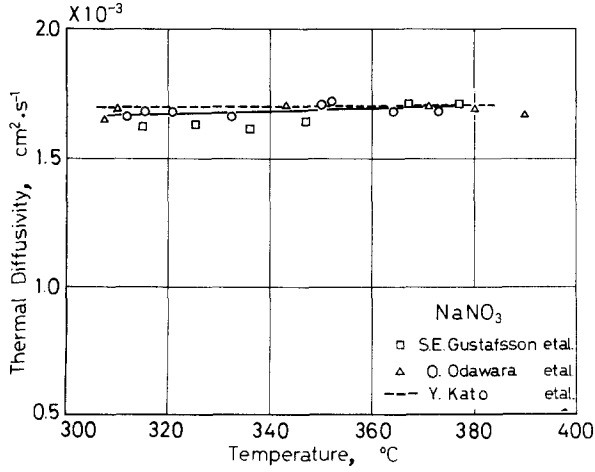

Fig. 20. Thermal diffusivity of molten sodium nitrate.

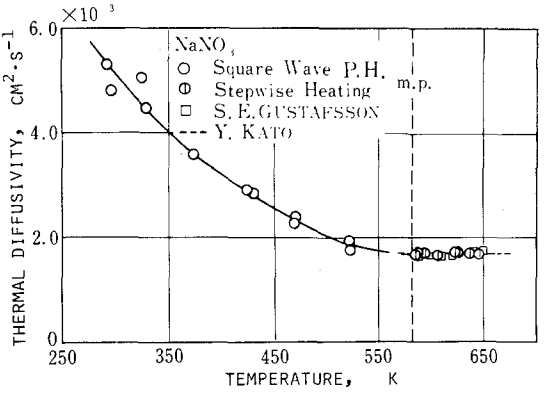

Fig. 21. Thermal diffusivity of $NaNO_3$ (including the data measured by the single rectangular pulse heating method in the solid phase).

the same as those of other researchers. For reference, the thermal diffusivity, combined with the data which were measured by the single rectangular pulse heating method in the solid phase, is shown in Fig. 21 [20], where Square Wave P.H. means the single rectangular pulse heating method.

ACKNOWLEDGMENTS

The author would like to express his thanks to Prof. Kiyosi Kobayashi of Shizuoka University and Dr. Yoshio Kato of the Japan Atomic Energy Research Institute for their helpful discussions.

REFERENCES

1. K. Kobayasi and T. Kumada, *J. Atomic Energy Soc. Japan* **9**:58 (1967), Translated into English as *UK At. Energy Establ. Transl.* **68/5071**:1 (1968).
2. K. Kobayasi and T. Kumada, *Tech. Rept. Tohoku Univ.* **33**:169 (1968).
3. T. Kumada and K. Kobayasi, *J. Nucl. Sci. Tech.* **12**:154 (1975).
4. T. Kumada and K. Kobayasi, *J. Atomic Energy Soc. Japan* **11**:462 (1969).
5. K. Kobayasi and T. Kobayashi, *Trans. Japan Soc. Mech. Engrs.* **46**:1318 (1980).
6. K. Kobayasi and T. Takano, *Trans. Japan Soc. Mech. Engrs.* **48**:2026 (1982).
7. Y. Kato, K. Kobayasi, N. Araki, and K. Furukawa, *J. Phys. E* **8**:461 (1975).
8. Y. Kato, K. Kobayasi, N. Araki, and K. Furukawa, *J. Phys. E* **10**:921 (1977).
9. K. Kobayasi and N. Araki, *Proc. 5th Int. Heat Transfer Conf.*, Vol. V (Tokyo, 1974), pp. 247–251.
10. Y. Kato, K. Furukawa, N. Araki, and K. Kobayasi, *Proc. 3rd Japan Symp. Thermophys. Prop.* (Hamamatsu, 1982), pp. 57–60.
11. N. Araki and K. Natsui, *Trans. Japan Soc. Mech. Engrs.* **49**(441 B):1048 (1983).
12. N. Araki, M. Ochi, and K. Kobayasi, *Trans. Japan Soc. Mech. Engrs.* **49**:(441 B):1058 (1983).

13. R. D. Cowan, *J. Appl. Phys.* **32**:1363 (1961).
14. W. J. Parker, R. J. Jenkins, C. P. Butler, and G. L. Abbott, *J. Appl. Phys.* **32**:1679 (1961).
15. T. Kumada and K. Kobayasi, *J. Nucl. Sci. Tech.* **13**:315 (1976).
16. K. Kobayasi, *Proc. 1st Japan Symp. Thermophys. Prop.* (Tokyo, 1980), pp. 105–108.
17. Y. Kato, K. Furukawa, N. Araki, and K. Kobayasi, *High Temp.-High Press.* **15**:191 (1983).
18. J. W. Cooke, ORNL-4728 (1971), p. 41.
19. N. Araki and K. Natsui, Preprint Japan Soc. Mech. Engrs. No. 803-2 (1980), pp. 56–58.
20. K. Kobayasi, N. Araki, and Y. Iida, *Proc. 7th Int. Heat Transfer Conf.*, Vol. 6, (Munchen, 1982), pp. 467–472.
21. Y. Kato, N. Araki, K. Kobayasi, and A. Makino, 18th Int. Conf. Thermal Cond., Rapid City, (1983).